INVESTIGATION OF NANOSCALE PROFILE OF DIELECTRIC SURFACES WITH THE USE OF X-RAY SCATTERING TECHNIQUE

Victor E. ASADCHIKOV, Igor V. KOZHEVNIKOV,
Boris S. ROSHCHIN, Yuri O. VOLKOV, Arsen E. MUSLIMOV
SHUBNIKOV INSTITUTE OF CRYSTALLOGRAPHY, Moscow, Russia

There are two important problems in studying surface and thin film morphology: (a) quantitative analysis of roughness evolution under different treatments (growth, erosion, oxidation, annealing, etc.) and (b) extracting of information about depth-distribution of the dielectric constant. Nowadays, X-ray reflection (XRR) and X-ray scattering (XRS or GISAXS) techniques are gaining increasing interest in solving these problems. Short wavelength of radiation and a possibility to vary the penetration depth of X-rays from several nanometers in the total external reflection region up to several microns with increasing grazing angle of a probe beam allow us to investigate thin film or surface morphology with nanometer or even angstrom resolution both in depth and in lateral direction. It gives us a comprehensive tool for investigating surfaces and interfacial borders on the nanoscale level especially combined with Atomic-Force Microscopy (AFM). In this talk we discuss the advantages of X-ray reflection and scattering methods adapted to conventional laboratory X-ray source. Several examples for both isotropic and anisotropic surfaces are given below.

In contrast to mechanical and optical profilometry, and to atomic force microscopy (AFM), the XRS technique is an indirect method based essentially on the theory of interaction of X-rays with inhomogeneous interface and on the model used to describe the surface. According to first-order Perturbation theory the scattering diagram has the following form [1,2]:

$$\Pi(\theta) = \frac{1}{W_{inc}} \frac{dW_{scat}}{d\theta} = B(\theta_0, \theta, \lambda, \varepsilon) \cdot \mathrm{PSD}(\nu); \qquad \nu = \frac{1}{\lambda} \left| \cos\theta_0 - \cos\theta \right|, \tag{1}$$

where W_{inc} is the incident power, dW_{scat} is the power scattered into the angular interval $d\theta$, and the electrodynamics factor B is independent of the roughness parameters. Equation (1) is valid for both step-like variation of the dielectric function and model of a near surface layer where the density changes slowly.

PSD-function appears to be a valid description for statistical parameters of roughness.
Let's notice that AFM data is a 2D function of surface profile. It's easy to find an autocorrelation function of such profile:

$$C(\boldsymbol{\rho}) = \langle Z(\boldsymbol{\rho}_1) Z(\boldsymbol{\rho}_1 + \boldsymbol{\rho}) \rangle; \qquad \boldsymbol{\rho} = (x, y), \tag{2}$$

where $Z(\boldsymbol{\rho})$ describes surface profile.

In the case of isotropic surface it is possible to change coordinates into polar and perform angular averaging of an autocorrelation function:

$$C(\rho) = \frac{1}{2\pi} \int_0^{2\pi} C(\rho, \vartheta) d\vartheta; \qquad \rho = \sqrt{x^2 + y^2}; \qquad \vartheta = a\tan\left(\frac{y}{x}\right), \tag{3}$$

Cosine Fourier transform of the autocorrelation function (3) gives PSD-function:

$$PSD(\nu) = 4 \int C(\rho) \cos(2\pi\nu\rho) d\rho \tag{4}$$

In the case of anisotropic surface PSD and scattering diagram appear to depend from the azimuth angle. To perform proper comparison with XRS we need to rotate *x*-axis to the same angle and then perform calculation of PSD of the x-axis section of an autocorrelation function:

$$PSD(\nu_x) = \int_{-\infty}^{\infty} C(x,0) \cdot exp(2\pi i \nu_x x) dx \qquad (5)$$

In certain cases it can be useful to describe the surface quality by a single number or by a set of roughness parameters. For this purpose the well-known parameter is effective roughness:

$$\sigma_{eff}^2 = \int_{\nu_{min}}^{\nu_{max}} PSD(\nu) d\nu \qquad (6)$$

For our experimental setup the range of spatial frequencies is from $\nu_{min} = 0.05$ μm^{-1} to $\nu_{max} = 10$ μm^{-1}.

Figure 1 shows PSD-functions for 2 sitall substrates obtained experimentally by XRS and AFM techniques. The difference in polishing quality for these samples is evident. The effective roughness is about 5.1 Å for sample 1 and about 2.6 Å for sample 2. Figure 2 demonstrates PSD-functions of nanostructured sapphire substrate surface. The period of terrace-like structure is of about 110 nm. Functions measured by both techniques with three different azimuth angles. The azimuth angle equal 0 corresponds to the orthogonal position of terrace structure to the direction of the X-ray beam. Positions of peaks correspond to the spatial frequency of periodic structure on the surface. We can characterise the dispersion of a structure period making analysis of width of such peaks. For this sample the divergence is 4 nm by AFM and 14 nm by XRS. The difference between these values shows how the divergence raises together with the size of examination area. Typical size of examination area for AFM usually not exceeds 100x100 μm and for XRS it is of about 100 mm^2. Experimental results shown on figures 1 and 2 reveal good agreement between XRS and AFM methods.

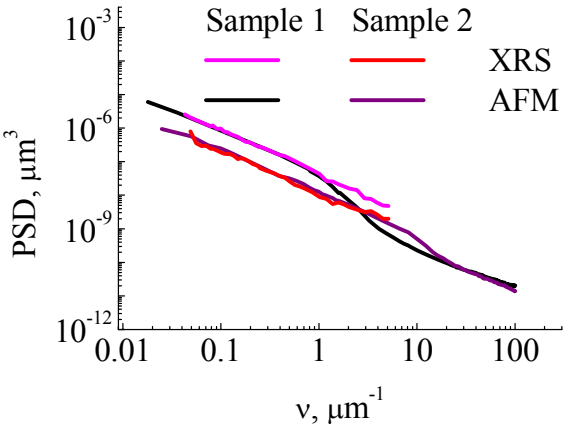

Figure 1. PSD-functions of sitall substrates. The average values of effective roughness: 5.1 Å for sample 1, about 2.6 Å for sample 2

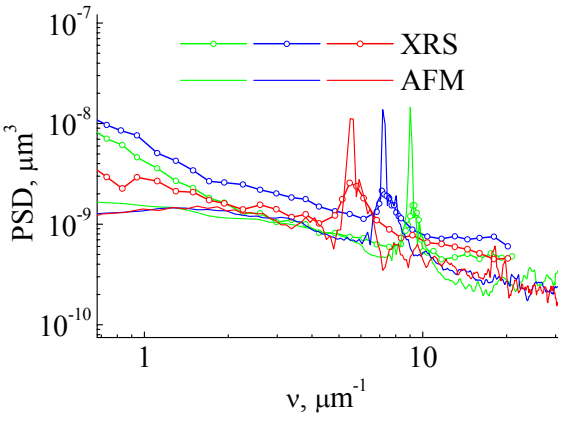

Figure 2. PSD-functions of nanostructured sapphire substrate measured with three different azimuth angles: 45 (red), 15 (blue) and 0 (green) degrees.

Similar to the case of a single surface, XRS diagram is connected with the statistical properties of the interface roughnesses by means of the 1D-PSD functions $PSD_{ij}(\nu)$, which are cosine Fourier transformations of the autocorrelation functions $C_{ij}(\rho)$ [3]:

$$\Pi(\theta) = \frac{1}{W_{inc}} \frac{dW_{scat}}{d\theta} = B_{11}(\theta_0,\theta)PSD_{11}(\nu) + B_{22}(\theta_0,\theta)PSD_{22}(\nu) + B_{12}(\theta_0,\theta)PSD_{12}(\nu) \qquad (7)$$

$$PSD_{ij}(\nu) = 4\int C_{ij}(\rho)\cos(2\pi\nu\rho)d\rho\,;\; C_{ij}(\rho) = \langle z_i(\rho_1) z_j(\rho_1+\rho)\rangle,\quad i,j=1,2;\quad \nu = \frac{1}{\lambda}|\cos\theta - \cos\theta_0|,$$

where the random functions $z_j(\rho)$ (j=1,2) describe profiles of vacuum-film and film-substrate interfaces. The electrodynamics factors B_{ij} in eq. (7) are independent of the roughness parameters. Figure 3 illustrates our approach to extraction of three 1D PSD functions of 5.5 nm thick Mo film roughness from a set of XRS diagrams measured at different grazing angles of a probe beam. The functions PSD_{22} and PSD_{11} describe the substrate and the film roughness, while the function PSD_{12} characterizes the correlation between roughnesses of both film interfaces. Figure 4 demonstrates an excellent agreement between 2D PSD functions of the external surface of the sample deduced by XRS and AFM techniques. Finally, figure 5 shows the conformity coefficient characterizing the vertical correlation between film and substrate roughness. As seen, correlation decreases with increasing spatial frequency and increasing film thickness.

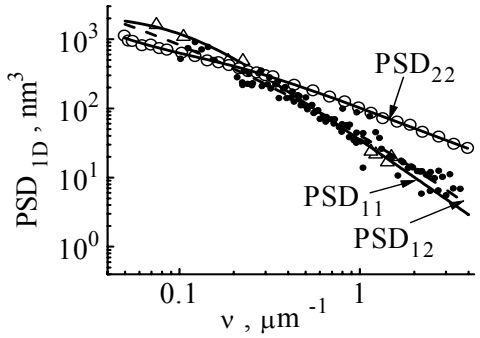

Figure 3. PSD-functions for 5.5 nm Mo film on Al_2O_3 substrates obtained by XRS.

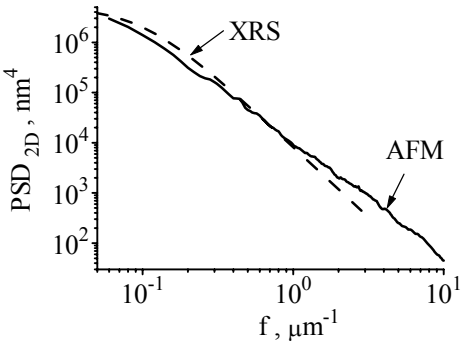

Figure 4. PSD-functions for external surface of Mo film.

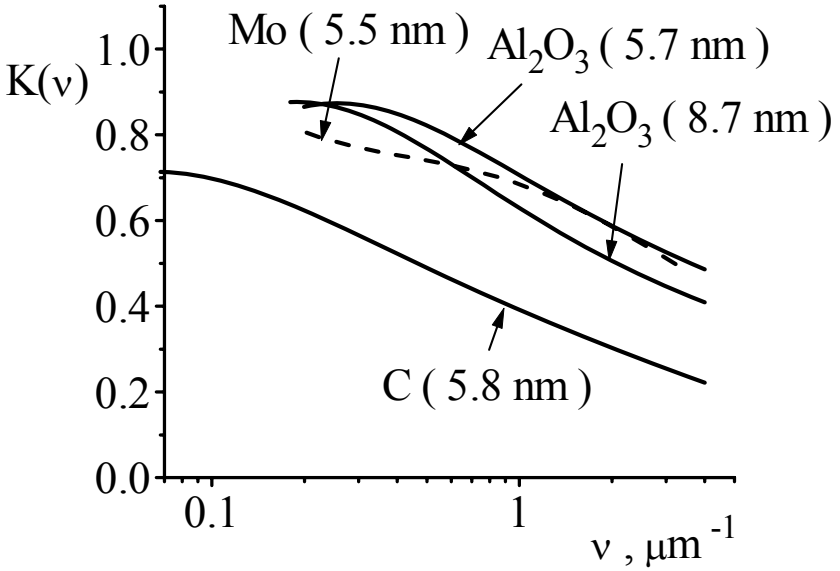

Figure 5. Correlation coefficient between Mo film and Al_2O_3 substrate roughness.

Several examples of the dielectric constant profile reconstruction based on the measured angular dependence of X-rays reflectivity [4] are presented in Figs.6-9. Figure 6 shows the measured reflectivity (circles) of Si_3N_4 film grown on Si substrate. The reconstructed profile of the dielectric constant is given in Fig.7. As seen, the quality of the film is very high and the film is characterized by the constant density and very sharp (i.e., very smooth) film-substrate interface. The only feature is a presence of about 2 nm thick adhesion layer on the sample top. The layer consists mainly of molecules of hydrocarbons, water and oxygen glued to the sample surface.

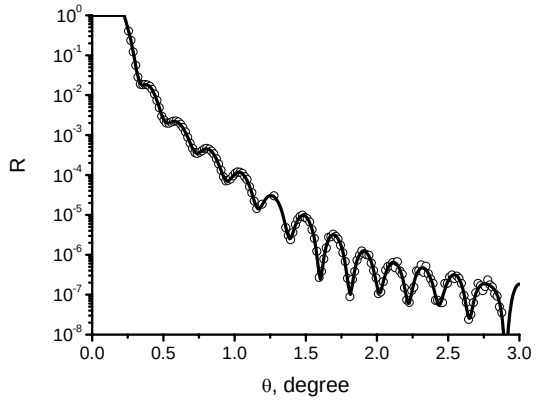

Figure 6. Reflectivity curves for Si_3N_4 film on Si substrate: experimental (circles) and simulated (line).

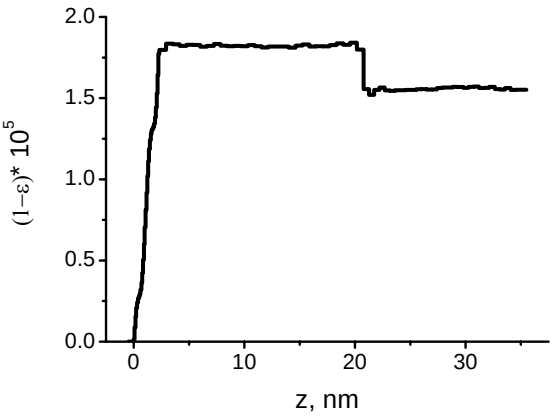

Figure 7. Reconstructed profile of dielectric constant for Si_3N_4 film on Si substrate.

In contrary, the measured reflectivity (Fig.8) and the reconstructed dielectric constant profile (Fig.9) of Al_2O_3 film deposited onto Si substrate by Atomic Layer Deposition technique demonstrate the film-substrate interface to be destroyed because of improper choice of the deposition conditions. Moreover, the film density varies essentially with depth.

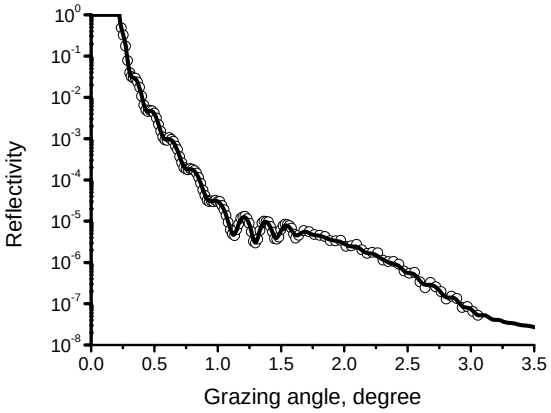

Figure 8. Reflectivity curves for Al_2O_3 film on Si substrate: experimental (circles) and simulated (line).

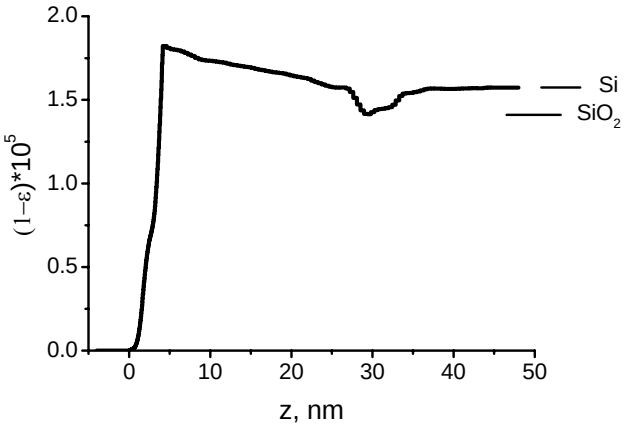

Figure 9. Reconstructed profile of dielectric constant for Al_2O_3 film on Si substrate.

Figure 10 demonstrate the variation of the reflectivity curve of the polished sapphire surface before (1) and after annealing at 1200°C during 1 h (2). For comparison the Fresnel reflectivity is also shown (3). The corresponding dielectric constant profiles are shown in Fig.11. As seen, annealing (curve 2) resulted in decrease of the density near the sample surface, what is consistent with Molecular Dynamics simulations [5].

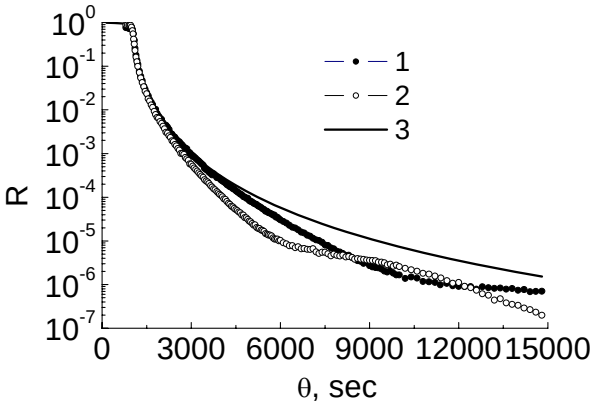

Figure 10. Experimental reflectivity curves for polished sapphire surface before (1), after annealing (2) and Fresnel reflectivity (3).

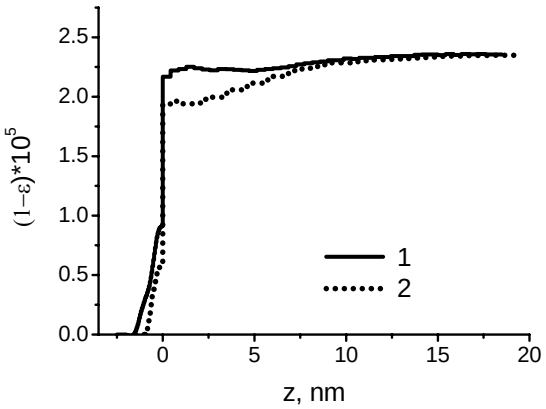

Figure 11. Reconstructed profiles of dielectric constant for for polished sapphire surface before (1) and after annealing (2).

Thus, the described X-ray investigation methods being non-destructive have the evident advantages in the study of the surface roughness and the interfaces. To our point of view they are also indispensable for the analysis of the depth-density distribution in the items.

References

1. A.V. Vinogradov, N.N. Zorev, I.V. Kozhevnikov, I.G. Yakushkin. About total external X-ray reflectivity effect // Journal of Experimental and Theoretical Physics (In Russian). 1985. Vol. 89. No. 6. Pp. 2124-2132.
2. E.L.Church, Fractal surface finish // Appl. Opt. 1988. Vol. 27. Pp.1518 – 1526.
3. V. E. Asadchikov, I. V. Kozhevnikov, Yu. S. Krivonosov. X-ray Studies of Thin-Film Coatings and Subsurface Layers of Solids // Crystallography Reports. 2003. Vol. 48. Suppl. 1. Pp. S37-S51.
4. I.V. Kozhevnikov. Physical analysis of the inverse problem of X-ray reflectometry // Nuclear Instruments and Methods in Physics Research A. 2003. Vol. 508. Pp. 519-541.
5. S. Blonski, S.H. Garofalini. Molecular Dynamics Simulations of α-aluminia and γ-aluminia Surfaces // Surface Science. 1993. Vol. 205. No. 1-2. Pp. 263-274.